Novel Microwave Bandpass Filter with Compact Size and Good Out-of-band Performance for Microwave Photonic Filter Applications

Johanny Escobar-Peláez[1], Jose-Luis Olvera-Cervantes[1], Ignacio E. Zaldívar-Huerta[1], Alonso Corona-Chávez[1], Alejandro García-Juárez[2], Jorge Rodríguez-Asomoza[3]
[1]Instituto Nacional de Astrofísica, Óptica y Electrónica (INAOE), Calle Luis Enrique Erro No. 1, Santa María Tonantzintla, Puebla, México, C. P. 72840
Email: johannyescobar@inaoep.mx
[2]Universidad de Sonora (UNISON). Depto. de Investigación en Física. Blvd. Luis Encinas y Rosales S/N, Hermosillo, Sonora, México, C. P. 83000
[3]Universidad de las Américas-Puebla (UDLAP), Depto. de Ingeniería Electrónica, Ex-hacienda Sta. Catarina Mártir, Cholula, Puebla, México, C. P. 72820

Abstract— **In this paper a novel microwave bandpass filter (BPF) with extended out-of-band rejection is presented. The BPF structure is based on a novel reduced size microstrip resonator which consists of two parallel lines in combination with a short-circuited stub. A BPF operating at 1.85 GHz with 11.11% fractional bandwidth (FBW) is designed, simulated and fabricated. Excellent agreements between simulated and experimental results were obtained. The electrical characteristics of the fabricated BPF allow its use in a microwave photonic filter (MPF) demonstrating in this way a practical application.**

I. INTRODUCTION

In microwave systems, a high performance as well as small size bandpass filters is essentially required to enhance the system performance and to reduce the fabrication cost. The size of microwave components is mainly related to the operating frequency, used materials and fabrication technology. In this context, numerous efforts have been conducted to reduce the size of BPF´s allowing improving the out-of-band response [1–6].

On the other hand, a microwave photonic filter (MPF) is defined as a system capable to carry out similar tasks to those of a microwave electrical filter. However, the main difference resides that a MPF allows the interaction between microwave RF signals and optical signals directly in the optical domain [7]. The use of a BPF brings supplementary advantages inherent to photonics such as low loss, high bandwidth, immunity to electromagnetic interference (EMI), and tunability. A BPF finds applications on satellital, cellular, radio, optical communications, instrumentation, etc.

Taking into account the concepts described before, in first place, this paper describes the design, simulation, and fabrication of a novel BPF. The main innovation of this work resides in that the BPF is based in a novel compact size resonator with high spurious frequency. In second place, a practical application of the fabricated BPF is demonstrated when the filter is placed at the output of a MPF in order to improve its frequency response. In summary, we propose and experimentally demonstrate the performance of the novel BPF operating in the microwave frequency range. The remainder of this paper is organized as follows. Section II describes the resonating structure along with the design of the microwave band-pass filter. Section III, is devoted to explain the topology and basic operation of the MPF used in this work, emphasizing in its frequency response. Simulation and experimental results are presented in Section IV. Finally, conclusions are summarized in Section V.

II. THE RESONATING STRUCTURE AND DESIGN OF A 4 POLE CHEBYSHEV FILTER

Fig. 1(a) illustrates the proposed novel resonator that consists of three microstrip transmission lines exhibiting a characteristic impedance of Z_0=50 Ω and an electrical length of 35° at the central frequency. The resonant frequency for the resonator structure can be determined considering the denominator for the expression used to compute the input impedance given as [8].

$$Z_{inr} = (1 + Z_s Y_{22})/(Z_s \Delta Y + Y_{22}) \quad (1)$$

Where

$$\Delta Y = (2/Z_{0L})^2 \quad (2)$$

$$Z_s = jZ_{0s} tan(\theta_s) \quad (3)$$

$$Y_{22} = -(2j/Z_{0L})cot(\theta_L) \tag{4}$$

Where Z_{0s} and Z_{0L} are the characteristic impedance corresponding to the stub and the parallel lines, respectively. θ_s and θ_L are the electrical length corresponding to the stub, and the parallel lines, respectively.

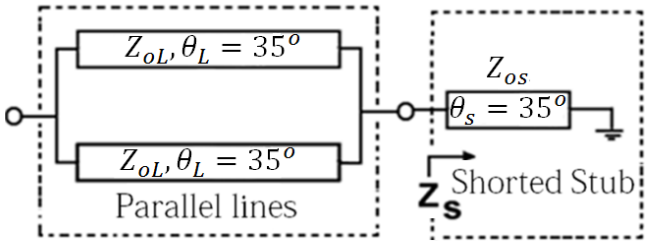

(a)

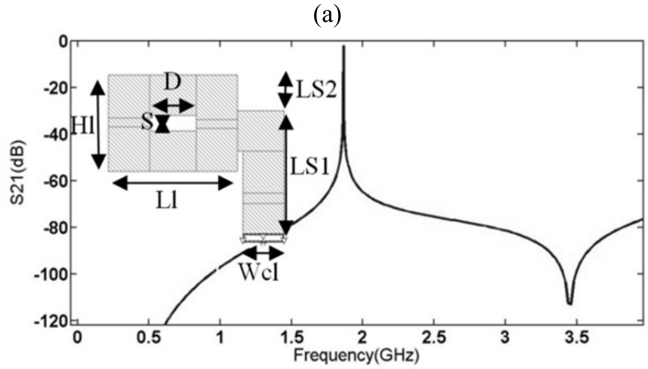

(b)

Figure 1(a) Proposed resonator, and (b) response of a single uncoupled resonator designed at 1.85 GHz.

A resonator was designed to operate at a central frequency of 1.85 GHz considering a substrate with $\epsilon_r = 4.34$ and h=1.5 mm. Fig. 1(b) corresponds to the simulation result obtained by the use of SONNET software [9]; it can be noticed that the resonant frequency was successfully obtained. Dimensions of the resonator are shown in Table I.

TABLE I. DIMENSIONS OF THE PROPOSED RESONATOR AT 1.85GHZ.

Dimensions of the resonator (mm)						
Hl	Ll	Wcl	LS1	LS2	D	S
6.7	9.1	2.9	8.5	2.5	3.3	1.1

The designed resonator occupies an area of 143.84 mm^2 which is 3.44 times lower than a 360° conventional closed loop resonator. Is worthy to mention that in the designed resonator the shorted stub is out of the two parallel lines; however, a substrate with higher permittivity allows introducing the shorted stub inside the two parallel lines and thus a quite compact filter can be obtained. By using the proposed resonator a fourth order Chebyshev filter designed to operate at 1.85 GHz and exhibiting a value of 11% of FBW was designed. The values for a low pass Chebyshev filter of fourth order exhibiting 0.1 dB ripple are: g_0=1, g_1=1.1088, g_2=1.3061, g_3=1.7703, g_4=0.8180, g_5=1.3554 [8]. Whereas couplings coefficients can be extracted as

$$Q_{ext1} = g_0 g_1/FBW\,, \qquad Q_{extn} = g_n g_{n+1}/FBW \tag{5}$$

$$M_{ij} = FBW/\sqrt{g_i g_j} \tag{6}$$

Where Q_{ext1} and Q_{extn} are the required external couplings coefficients for the first and last resonator, respectively. M_{ij} are the required mutual coupling coefficients between resonators. Thus, the required coupling parameters are: Q_{ext1}=10.2564, Q_{ext2}=10.2556, M_{12}=0.09, M_{23}=0.0711 and M_{34}=0.898. The practical external coupling coefficients can be calculated by using [10]

$$Q_e = f_0/\Delta_{FBW} \tag{7}$$

Where the 3 dB frequency band width (Δ_{FBW}), and the central frequency (f_0) are computed from full wave simulations of the structure shown in Fig. 2(a). External coupling coefficients depend mainly on the length (L) and the gap (Se1). On the other hand, the practical mutual coupling coefficients between resonators are calculated as

$$M_{ij} = (f_2^2 - f_1^2)/(f_2^2 + f_1^2) \tag{8}$$

Where f_1 and f_2 are the corresponding resonant frequencies obtained from the simulated scattering parameters of the two topologies shown in Fig. 2(b) and 2(c). The mutual coupling coefficients depend on the distances d12 and d23.

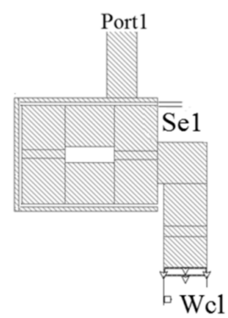

(a)

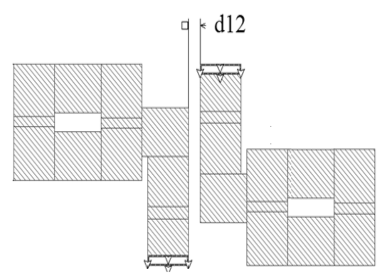

(b)

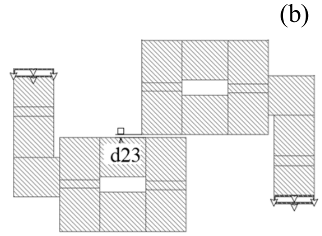

(c)

Figure 2. (a) External coupling structure, (b) first and (c) second topology to determine the mutual coupling between resonators.

Fig. 3 corresponds to the final layout of the designed filter. The desired external couplings were achieved by means of a transmission line with a width of 0.2 mm and length of 24.5 mm that is coupled to the resonator by means of a gap (se1) of 0.2 mm. It is also seen that the topology 2 (Fig. 2(c)) was used to obtain the coupling coefficient M_{23} whereas that the topology 1 (Fig. 2(b)) was employed to achieve the coupling coefficients M_{12} and M_{34}. In this case, d12=0.8mm, d23=0.2mm and d34=0.8mm.

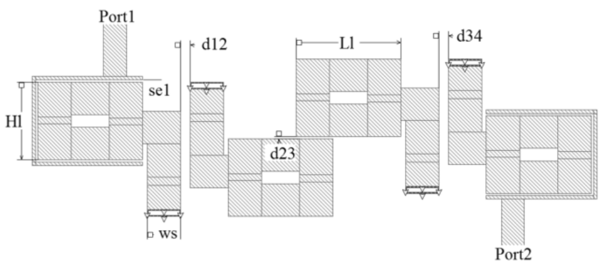

Figure 3. Final layout of the prototype at 1.85 GHz

III. The Microwave Photonic Filter

As has been previously reported in [11], the frequency response of the electro-optical system depicted in Fig. 4 is determined by the real part of the Fourier transform of the optical spectrum of the Multi-Longitudinal Laser Diode (MLLD) utilized. The use of this electro-optical system allows filtering of signals in the frequency range of the microwaves.

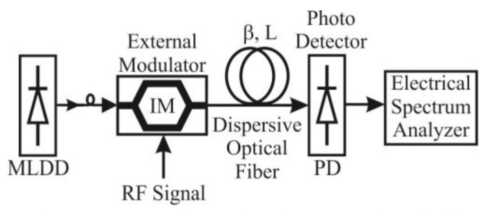

Figure 4. Scheme corresponding to the microwave photonic filter (MPF) used to obtain filtering of microwave signals.

Its frequency response includes a low-pass band centered at zero frequency and multiple bandpass windows, centered at the central frequency given as

$$f_n = n/DL\delta\lambda \tag{9}$$

where the associated bandwidth of each bandpass window is

$$\Delta f_m = \left(2\sqrt{ln2}\right)/(\pi DL\Delta\lambda) \tag{10}$$

In expressions (9) and (10), D is the chromatic fiber-dispersion parameter in ps/nm-Km, L is the length of the optical fiber in kilometers, $\delta\lambda$ is the free spectral range between two adjacent modes of the MLLD in nanometers, $\Delta\lambda$ is the full width at half maximum (FWHM) of the spectrum of the optical source given in nm, and n is an integer (n = 1, 2,…). A typical frequency response of the MPF considering L=28.3 km of single-mode standard optical fiber exhibiting a chromatic fiber-dispersion parameter D=17 ps/nm-km at 1550 nm, $\delta\lambda$ =1.1 nm, and $\Delta\lambda$=4.96 nm is illustrated in Fig. 5. It is clearly appreciable the presence of a lowpass band and two bandpass windows centered at 1.85 GHz and 3.8 GHz. These last values are in good agreement according to Eq. (9), because the bandpass windows occur at integer multiples of the central frequency response f_n. The goal to use the fabricated BPF is to suppress the lowpass band and the second bandpass window. Precisely, the inclusion of the BPF on the structure of the MPF will allow select and "sharpen" only the bandpass window located at 1.85 GHz.

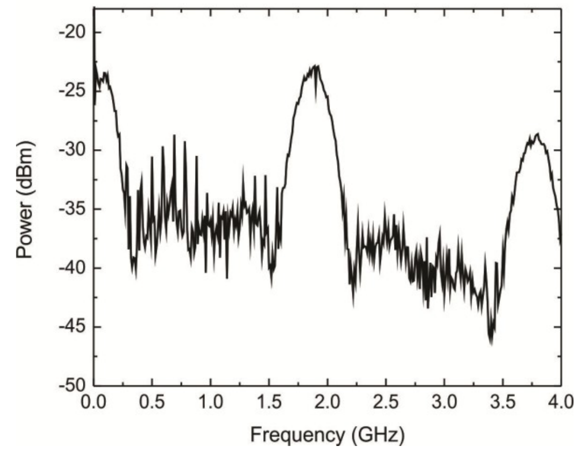

Figure 5. Experimental frequency response of the MPF

IV. Simulations And Experimental Results

This section is divided into two subsections. In the first subsection, the simulations and experimental results corresponding to the BPF are presented. Next, in the second subsection, it is described the experimental results corresponding to the use of the BPF in the MPF setup.

A. Simulations and experimental results

Fig. 6 shows a picture of the fabricated BPF where SMA connectors have been welded in order to allow that the BPF can be connected with other devices. Its physical dimensions were 23x54 mm^2.

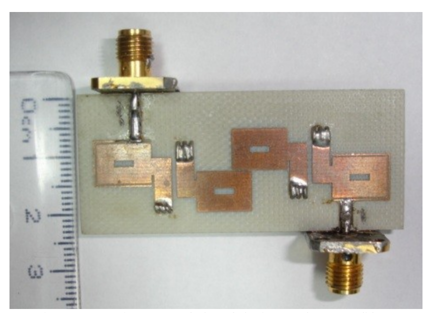
Figure 6. Picture of the fabricated BPF filter

In a first step, simulated and measured S-parameters were obtained by using Sonnet software and by a Vector Network Analyzer (VNA, model E8361A), respectively. Fig. 7 plots both results in order to be compared. Simulated and experimental FBW are 11.7% and 11.11%, respectively. Insertion loss is 4.05dB±0.85dB, and returns loss is better than 10dB within the measured bandwidth. In Fig.7 (a) it is clearly appreciable that the first spurious frequency is located around 6GHz and 6.6 GHz, corresponding to the simulated and measured value, respectively. In the first case, this value corresponds to 3.24 times the frequency of interest, whereas for the second case corresponds to 3.58 times. As can be seen in Fig 7(b), a very high out-of-band attenuation was obtained.

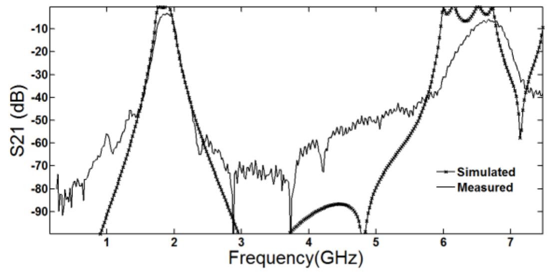

(a)

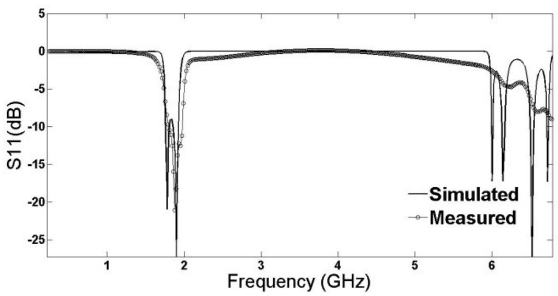

(b)

Figure 7. Simulated and measured results. (a) S_{21} parameters (b) S_{11} parameters

B. A practical application of the electrical BPF

How it was established at the beginning of this paper, a practical application of the BPF fabricated resides into improve the frequency response of a Microwave Photonic Filter. For this goal, the configuration shown in Fig. 8 was experimentally assembled in the laboratory.

It is clearly remarkable the insertion of the BPF into the electro-optical set-up

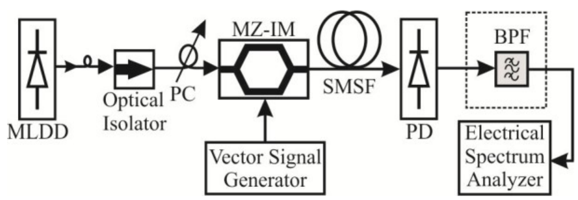

Figure 8. Setup of the Microwave Photonic Filter showing the inclusion of the electrical BPF.

The operation principle of this scheme is the follows: The optical source used in this experiment was a MLLD (Thorlabs, model LPS-1550-FC), emitting at 1550 nm that was optically characterized by means of an Optical Spectrum Analyzer (Agilent, model 86143B), obtaining $\delta\lambda$=1.1 nm for a drive current of 19 mA. At the output of the MLLD an optical isolator was placed in order to avoid reflections to the optical source and then a polarization controller (PC) was used for controlling the phase. The optical signal was launched into a Mach-Zehnder intensity modulator (MZ-IM). The microwave electrical signal for modulating the optical intensity was supplied by a Vector Signal Generator (VSG, Agilent E4438C). The intensity modulated optical signal was then coupled into a 28.3 km of single-mode standard optical fiber coil exhibiting a value of D=16.671 ps·nm^{-1}km^{-1} at 1550 nm. At the end of the link, the optical signal was applied to a fast photo-detector (PD, Miteq DR-125G-A), next the fabricated BPF was placed. Finally, the output of the BPF (inside dotted box) was connected to an Electrical Spectrum Analyzer (ESA, Agilent E4407B) in order to measure the frequency response of the complete electro-optical system. The measured frequency response of the MPF in the frequency range of 0-4 GHz without the use of the fabricated BPF is illustrated in Fig. 9 (dashed line). It can be seen that the first bandpass window of the photonic filter system occurs at 1.85GHz whereas that the second bandpass window is located around 3.8GHz. Continuous line correspond to the measured frequency response when the fabricated BPF is used. It is clearly appreciable that both the low frequency range (under 500MHz) as well as the high frequency range (around 3.8GHz) are annulled due to the good out-of-band performance of the developed filter.

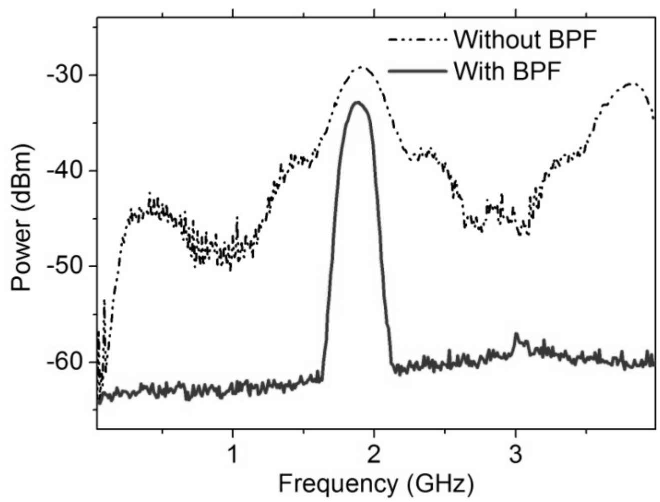

Figure 9. Measured frequency response of the MPF showing the effect of the fabricated BPF

V. Conclusion

A novel BPF with good out-of-band performance was presented. The electrical filter is based on a novel reduced size microstrip resonator. A prototype at 1.85 GHz with 11.11% fractional bandwidth was designed, simulated, and measured. Excellent agreement between simulations and measurements data were obtained. The filter was made using the traditional full wave simulation method. The main advantages of proposed filter are its reduced size and its high spurious frequency. Finally, a practical application of the fabricated BPF was achieved. For this goal, the BPF was inserted into the structure of a MPF in order to suppress undesirable bands. Experimental results showed a substantial improvement on the frequency response of the MPF. As a future work, impact of variability in the substrate manufacturing and tolerances on the filter response will be carried out in order to improve its behavior. At the same time, transmission of data using the filtered bandpass windows as electrical carrier can be done.

ACKNOWLEDGMENT

One of the authors, Johanny Escobar-Peláez thanks to the Mexican Consejo Nacional de Ciencia y Tecnología (CONACyT) for the scholarship number 374152.

REFERENCES

[1] X. Lu, X Guo, S.Jin, X. Zhang, H. Peng, M. Li, B.Wei, B Cao, "UHF band ultra-narrowban superconducting filter with double U-Type secondary coupling structure", IEEE microwave and wireless components letters, vol. 19, No. 11, November 2009.

[2] Zhou, J Lancaster and F. Huang, "Superconducting Microstrip Filters Using Compact Resonators with Double-Spiral Inductors and Interdigital Capacitors", Microwave Symposium Digest, 2003 IEEE MTT-S International, Vol.3, June 2003

[3] F. Huang, M. Zhou and L. Yue, "A Narrowband Superconducting Filter Using Spirals With a Reversal in Winding Direction", IEEE transactions on microwave theory and techniques, vol. 54, NO.11, November 2006.

[4] S. Jin, B Wei, B.Cao, X. Zhang, X. Guo, H. Peng, Y. Piao, B. Gao "Desigh and Performance of an Ultra-Narrowband Superconducting Filter at UHF Band", IEEE microwave and wireless components letters, vol. 18, No. 6, June 2008.

[5] A. Afkhami, M. Tayarani, "Spurious Response Suppression in Hairping Filter Using CSRR Merged In The Filter Structure", Progress In Electromagnetics Research C, Vol. 11, 137-146, 2009.

[6] L. Ying, H. Zheng, "A Miniaturized Narrowband Bandpass Filter with Wide Stopband Using Open-Loop Resonator", Microwave and optical technology letters, vol. 53, No. 9, September 2011.

[7] J. Capmany, "A Tutorial on Microwave Photonic Filters", IEEE Journal of lightwave tecnology, Vol. 24, No. 1, January 2006.

[8] George L. Matthaei, Leo Young, E.M.T. Jones, "Microwave filters, impedance-matching networks, and coupling structures", Artech House, 1980.

[9] Sonnet EM full-wave simulator.

[10] Jia-Sheng, M.J. Lancaster "Microstrip filters for RF/Microwave applications", John Wiley & Sons, INC, 2001.

[11] G. Rodriguez, I. Zaldívar, J. Rodriguez, A. García, P. Rubio, "Modeling and perfomance analysis of an all-optical photonic microwave filter in the frequency range of 0.01-15 GHz, Proc. Of SPIE Vol. 7620 76200B-1, 2010.